Traffic Reduction and Decarbonization through Network Changes - Empirical Evidence from Paris

Elena Natterer*
Chair of Traffic Engineering and Control, Technical University of Munich, Germany
Email: elena.natterer@tum.de

Allister Loder
Chair of Traffic Engineering and Control, Technical University of Munich, Germany
Email: allister.loder@tum.de

Klaus Bogenberger
Chair of Traffic Engineering and Control, Technical University of Munich, Germany
Email: klaus.bogenberger@tum.de

* Corresponding author

Word count: 5853 words + 3 table(s) $\times$ 250 + 750 words for references = 7353 words
Submitted: April 16, 2024

Paper submitted for presentation at the 103rd Annual Meeting Transportation Research Board, Washington D.C., January 2024

ABSTRACT

Over the past years, Paris, the capital of France, has experienced notable changes in its road network supply: the city has reduced space dedicated to cars while concurrently expanding dedicated infrastructure for active modes of transportation. This policy aims to reduce car travel and its externalities, like carbon emissions. The Downs-Thomson paradox provides a hypothesis to which extent this modal shift occurs: assuming that road networks is reduced and average cycling door-to-door journey times improve, it could be expected that car travel reduces to a level that leads to similar or less congestion than before the intervention.

In this paper, we investigate the relationship of car network reduction and bike network expansion with reduced car travel and increased bike travel. We use empirical traffic data from Paris as well as map data from OpenStreetMap for the time period from 2015 to 2022. The results reveal a significant shift: car traffic declined by approximately 13%, inflow car traffic by 23%, and cycling increased 94% from 2016 to 2022 (cycling was not measured in 2015). We use the theory of the macroscopic fundamental diagram (MFD) to assess the change in traffic behaviour. Comparing the MFDs from 2015 to 2022, the MFD capacity is reduced by about 15%. Overall, we find that the decline in car travel reduced carbon emissions by 11%. Considering Paris' reputation as a progressive city in terms of network supply re-adaptation, the outcomes of this study hold relevance for all cities currently engaged in transport supply adjustments.

Keywords: network changes, traffic data, Paris bike network, network/macroscopic fundamental diagram; Down/Thomson paradox; decarbonization

INTRODUCTION

There are many cities notable for their transportation system, while one city is, in particular, notable for its transformation of the transportation system: Paris, the capital of France. Paris massively changed and is continuing to change its road network supply: reducing the space available for the car, and expanding the space for the bike. Some view this and similar initiatives in France as a step towards making France a global leader in promoting cycling (*1*). This transport policy aims at discouraging car use and promoting cycling and thus supporting Paris' decarbonization goals. By 2050, Paris plans to completely eliminate local emissions, making the city emission-free. Additionally, they aim to reduce the carbon footprint by 80% compared to 2004 levels (*2*).

The transformation in Paris can be attributed to various political initiatives introduced from 2015 onwards, largely led by Mayor Anne Hidalgo (2014 -). Notably, the Plan Velo I (2015 - 2020) and Plan Velo II (2021 - 2026) have played a significant role in making Paris a more bike-friendly city, with the objective of achieving a "100% cyclable" status (*3*). During the implementation of these plans, approximately 1,000 km of bike paths were created between 2015 and 2020, with plans to add an additional 180 km by 2026 (*4, 5*). The second plan also includes the removal of 72% of car parking spaces (*6*). Other initiatives, such as "Paris breathes" since 2016, involve temporary street closures on Sundays, and the city's transformation towards becoming a "15-minute city" since 2020. This transformation encompasses conceptual changes, such as repurposing school playgrounds into parks after hours, and network changes, including redesigning public squares like Place de la Bastille to include trees and bike lanes (*7*). The main objective of these initiatives is to improve bike accessibility and promote sustainable transportation options city-wide. The collective efforts aim to create a greener, pedestrian-friendly urban environment and make Paris more conducive to cycling. As a result of the Plan Velo I, Plan Velo II, and the alterations towards becoming a "15-minute city", the bike and car network in Paris has undergone significant changes. Consequently, it is not feasible to evaluate the impact of each plan in isolation; we must consider the overall network changes since 2015.

Paris serves as a compelling example for many cities facing the challenges of achieving emission targets amid the climate crisis. Understanding the impact of significant network modifications on transportation behavior becomes crucial as cities consider changes and promote cycling. Additionally, Paris' substantial investment in Velo I and Velo II (over 400 million euros) highlights the importance of analyzing changes to aid budget planning. Valuable insights from Paris' network changes can inform expectations of traffic behavior adjustments in other cities.

All the changes to the network lead to the question of to which extent the politically desired modal shift occurs. Here, the Down/Thomson paradox provides a starting point (*8*–*10*): the removal of car space reduces the overall network capacity, i.e., increasing door-to-door journey travel times for cars with everything else being equal, while improved cycling infrastructure decreases cycling door-to-door journey travel times in addition to the safety benefit. Consequently, a new equilibrium point can be expected where car travel is reduced by that amount which leads to similar or less congestion compared to the time before the intervention. Less congestion can be expected as cycling travel times improve over the years. However, considering the changes in travel preferences since the COVID-19 pandemic, e.g., working from home and cycling (*11, 12*), it is likely that these changes also affect the observed traffic outcomes in Paris, i.e., leading to a different equilibrium than expected based on the prediction of the Down/Thomson paradox. Nevertheless, in this paper, we investigate the relationship between network changes and demand changes and their implications on decarbonization. Our analysis of to which extent supply-side measures are an

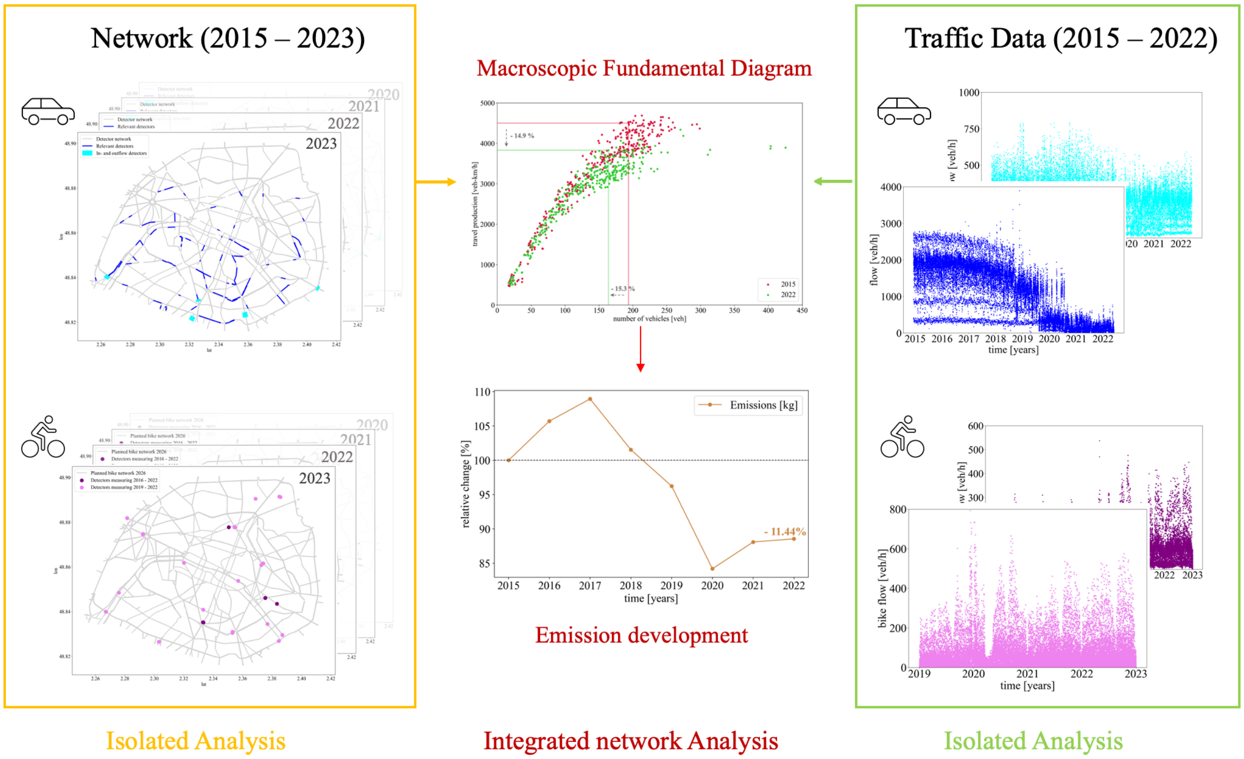

FIGURE 1 : Overview of workflow

effective means of transportation demand management uses empirical car and bike traffic data from Paris for the time period from 2015 to 2022 as well as historical map data from OpenStreetMap together with the theory of the macroscopic fundamental diagram (MFD). It provides a macroscopic and aggregated perspective of traffic in an entire urban network (*13*) and is consequently appropriate for assessing Paris' transport policy.

This paper contributes with the first large-scale empirical assessment of network changes and changes in bike and car traffic flow in Paris. The data-driven analysis reveals that traffic production has decreased by 13%, and the inflow travel production by 23%, while the car network decreased by 5% (lane km) during our observation period. Congestion levels also appear to have fallen. In contrast, bike traffic increased by 57% for those detectors installed in 2019, and even 94% for those installed in 2016, while the bike network increased by 11%.

This paper is organized as follows and as illustrated in Figure 1. The next section presents the methods used for the assessment. Then, we present the processing of the network and traffic data, followed by the results. In the last section we provide a conclusion that highlights the novel insights gained, limitations of the proposed method, and future research directions.

METHOD

We explore the impact of car and bike network changes on the respective car and bike traffic in Paris using the theory of the macroscopic fundamental diagram (MFD) (*13*, *14*) as well as measured network changes from OpenStreetMap (see next section). The MFD provides an aggregated macroscopic and network-wide relationship between the number of vehicles in the network and the average speed of all vehicles in the network. This relationship results from network topology and

TABLE 1 : List of symbols used in this analysis.

Symbol	Unit	Description
Y	-	Set of years with elements $\{2015;\ldots;2023\}$
y	-	Year index
D_y	-	Set of all days in the considered year y
D	-	Union of all sets D_y for all years $y \in Y$
d	-	Day index
H	-	Set of hours in the day (24-hour clock) with elements $\{5;\ldots;22\}$
h	-	Hour index
N_c	-	Set of network car detectors
$N_{c,inflow}$	-	Set of inflow car detectors
N_b	-	Set of bike detectors
i	-	Detector index
o_{ihd}	%	Detector occupancy
q_{ihd}	veh/h	Flow of vehicles (cars or bikes) per hour
l_i	km	Length of the road segment of car detector $i \in N_c$
$L_{c,y}$	lane-km	Length of the total road network in lane-km, for given year y
$L_{b,y}$	cycleway-km	Length of the total bike network in cycleway-km, for given year y
u_f	km/h	Observed free-flow speed in Paris
Π_{hy}	veh-km/h	Travel production per hour h and year y
v_{hy}	km/h	Velocity per hour h and year y
$e(v)$	kg/10 km	Speed-specific emissions
E_y	kg	Emissions per year $y \in Y$

multimodal traffic operations (*15*–*18*). The network-wide perspective provides a unique opportunity to assess the impact of large-scale transport policies such as re-purposing road space (*19*), changing routes (*20*), or changing the headway of the bus system (*21*). The MFD distinguishes three types of flows: internal flows, network inflow, and network outflow. While the first flow captures all vehicle movements inside the network, which is described by the MFD, the network inflow describes the number of vehicles that are entering the network per unit of time. Conversely, the network outflow summarizes all vehicles that leave the network or end their trip in the network. Based on the average network speeds estimated in the MFD, we can use speed-specific carbon emission factors to compute the total carbon emissions, following the idea of emission-macroscopic fundamental diagram (*22*). Table 1 lists all symbols used in this analysis.

The MFD can be estimated with various methods (*23*), but considering the focus on assessing empirical changes of Paris' urban-scale transport policies over a long period of time, only the "loops method" seems appropriate. Loop detectors are built into the street and count the number of passing vehicles per unit of time, flow q in vehicles per hour, and the time that vehicles occupy the detector, occupancy o in percent. Flow and occupancy are recorded in Paris at every measurement location $i \in N_c$, in every hour $h \in H$, on every day $d \in D$. Note that loop detectors are usually not installed on all roads, but only on a subset of roads, here denoted N_c. The assumption is made that these roads are representative for the entire considered network. In this analysis, we select the MFD representation of travel production Π versus the number of vehicles n because the flow data reported in Paris is for the entire link, not per lane, and we have no information on the number of lanes per measurement location; hence, we cannot express the MFD on a per-lane basis.

We estimate the macroscopic fundamental diagram as follows. First, we aggregate the occupancy of all single detectors o_{ihd} to the network average occupancy o_{hd} as shown in Eqn. 1.

$$o_{hd} = \frac{1}{|N_c|} \sum_{i \in N_c} o_{ihd} \quad \forall h \in H, \forall d \in D \tag{1}$$

Second, the total travel production of all detectors Π_{hd} is calculated using the detector flow q_{ihd} and its associated road network length l_i as shown in Eqn. 2.

$$\Pi_{hd} = \sum_{i \in N_c} l_i q_{ihd} \quad \forall h \in H, \forall d \in D \tag{2}$$

Average network occupancy o_{hd} can be transformed into the accumulation of vehicles n_{hd} using a linear transformation with scalar s (*14, 24*). We obtain a reliable estimate of s for Paris by calibrating the MFD's free-flow branch to speed values reported for the periods in which traffic states are in the interval of 0 to 4% occupancy. We find that the average free-flow speed in Paris is around $u_f = 28\,\text{km/h}$ (*25*). Using the fundamental equation of traffic flow $v = \Pi/n$ (*26*), we can express the relationship between the measured Π_{hd}, o_{hd} and u_f values and the calibration scalar s as given in Eqn. 3.

$$u_f = \frac{\Pi_{hd}}{o_{hd}/s} \tag{3}$$

The best value for s is derived using ordinary least squares and is found to be $s = 0.046$. With the calibration scalar (s) determined, we transform all average network occupancy values o_{hd} into the number of vehicles n_{hd} and subsequently calculate the speed ($v = \Pi/n$) for all points in the estimated MFD.

Using the idea of the emission-MFD (*22*), we can use the estimated MFD as given in Π_{hd}, n_{hd}, and v_{hd} to derive average daily carbon emissions from the estimated MFD E based on speed-specified emission values $e(v)$. Table 2 lists the values used in this analysis.

TABLE 2 : Speed-specific emission values $e(v)$, taken from (*25*).

Speed [km/h]	Emissions [kg/10 km]
17.5	2.38
20.0	2.28
22.5	2.15
25.0	2.10
27.5	1.98
30.0	1.92

We estimate the average daily emissions E_y in year y as given in Eqn. 4, where Π_{hy} and v_{hy} are the annual average values of the observed travel production and accumulation values at hour h

in year y in the MFD, i.e., $\Pi_{hy} = \frac{1}{|D_y|}\sum_{d\in D_y}\Pi_{hd}$ and $v_{hy} = \frac{1}{|D_y|}\sum_{d\in D_y} v_{hd}$.

$$E_y = \sum_{h\in H} \Pi_{hy} \cdot e\left(v_{hy}\right) \quad \forall y \in Y \tag{4}$$

To quantify the network changes in Paris, we define three quantities. The capacity of the MFD C_y, the total network length of cars $L_{c,y}$ in lane-kilometres, and the total network length of bikes $L_{b,y}$ in cycleway kilometres in each year y. While the measurement of $L_{c,y}$ and $L_{b,y}$ uses map data (see next section), the MFD capacity is defined as the 95th percentile of the travel production of year y in the MFD as shown in Equation 5.

$$C_y = \Pi_{hd,[95]} \quad h \in H, d \in D_y \tag{5}$$

We define four quantities for each year y that measure the changes in car and bike traffic:

1. The average *travel production* in the network $\bar{\Pi}_y$:

$$\bar{\Pi}_y = \frac{1}{|D_y|}\sum_{d\in D_y}\sum_{h\in H}\Pi_{hd}, \tag{6}$$

2. The average *accumulation of vehicles* in the network $\bar{n}_y$:

$$\bar{n}_y = \frac{1}{|D_y|}\sum_{d\in D_y}\sum_{h\in H} n_{hd}, \tag{7}$$

3. The average *travel production of a selected number of inflow links* $\bar{\Pi}_{y,inflow}$:

$$\bar{\Pi}_{y,inflow} = \frac{1}{|D_y||N_{c,inflow}|}\sum_{d\in D_y}\sum_{h\in H}\sum_{i\in N_{c,inflow}} l_i \cdot q_{ihd}, \tag{8}$$

4. The average *bike counts* $\bar{B}_y$:

$$\bar{B}_y = \frac{1}{|D_y||N_b|}\sum_{d\in D_y}\sum_{h\in H}\sum_{i\in N_b} q_{ihd}. \tag{9}$$

Regarding this paper's hypotheses, we expect a positive correlation between the network's travel production ($\bar{\Pi}_y$) and the travel production of inflow detectors ($\bar{\Pi}_{y,inflow}$) with both the MFD capacity (C_y) and the total road network length ($L_{c,y}$). Conversely, we expect a slightly weaker positive correlation between vehicle accumulation ($\bar{n}_y$) and MFD capacity/road network length. Analogously, we anticipate a positive correlation between bike counts ($\bar{B}_y$) and the total length of the bike network ($L_{b,y}$).

NETWORK DATA

In this section, we discuss the derivation of the total network length for car and bike traffic in Paris. For each year $y \in Y$, $L_{c,y}$ notates the lane-kilometres for car traffic, and $L_{b,y}$ notates the cycleway kilometres of the bike-network. Current and historical data for the Paris car and bike

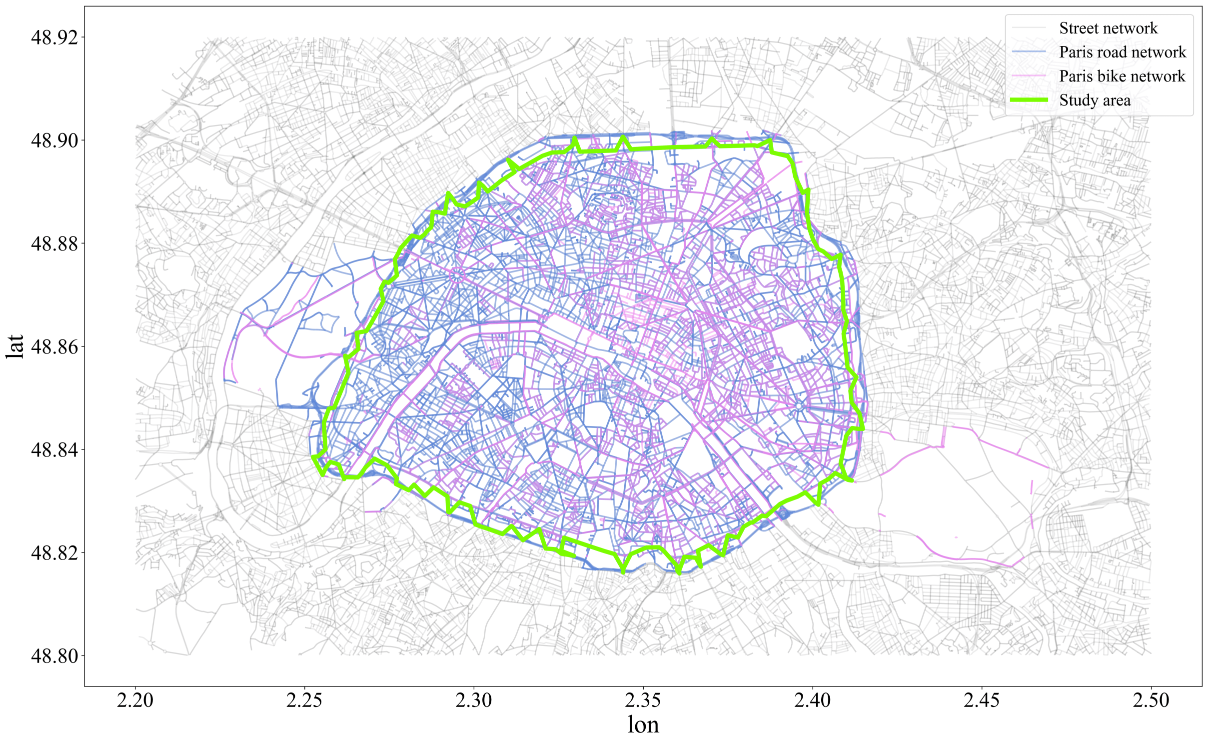

FIGURE 2 : Paris' road and bike network and the studied area

network is obtained from OpenStreetMap (OSM) (*27*) using OSMnx (*28*). In this analysis, we focus on the road network within the Boulevard Périphérique, a motorway ring road encompassing the entire city. This ring offers a natural boundary for studying changes on the supply and demand side. Figure 2 shows the selected networks, with the bike network highlighted in violet and the road network in blue, while the boundary of the study area is shown in green. These colors are consistently used for the two modes in the following. It is worth noting that both networks extend beyond the study area, reaching into the suburban regions outside the boundaries of Paris.

Technical procedure

To obtain the network data, we follow the following procedure: We request data from OSM, for January 1st of the years 2015 to 2023, for the region inside the Boulevard Périphérique (using the polygon option of OSMnx). Using the *graph_from_polygon* function with *simplify=False*, we preserve different road and cycleway classifications in order to examine edges based on their specific classifications. The *road classification* of an edge in the car network is the value in the column "highway": This value serves as the primary identifier for different types of roads, streets, or paths (*29*). Examples include "primary", "secondary" and "residential". We group edges with a road class ending on "_link" (i.e. "primary_link") into the "other" road classification. The *cycleway classification* of an edge in the bike network is determined by the value in the "cycleway" column. The "cycleway" attribute serves as the primary identifier for cycling infrastructure, encompassing cycle lanes that are part of the road and separated cycle tracks running parallel to the road (*30*). Examples are "opposite", "track", "lane", etc.

For the car network, computing the kilometres per edge classification is straightforward.

For the bike network in OSM, there is more space for interpretation compared to the car network: OSMnx provides an option to compute the total bike network using the parameter *network_type= "bike"*. This includes all streets where biking is theoretically possible, including roads with road classifications such as primary streets, etc. The total length of this network is 1,785 km in 2015 and 1,861 km in 2023. However, official statistics state the lengths as 740 km in 2015 and 1,400 km in 2020 (*4, 5*). To address this, we follow Geoffrey Boeing's suggestion, which is to consider a graph comprising everything with either a cycleway key or "highway=cycleway" tag. This involves permissively downloading more data than needed, removing non-cycleways, eliminating isolated nodes, and finally simplifying the graph's topology (*31*). We then filtered out edges with the bike classifications "no" or "none". The resulting bike network has a length of 1,072 km in 2015 and 1,126 km in 2020. This does not match precisely the city's official figures, however, we consider this network a better estimate than using the total bike map created with the parameter *network_type= "bike"*. These estimates are then considered the bike network length $L_{b,y}$ in year y.

We compute the lane-kilometres for the car network as follows: For every year, we first group the edges by their road classification and compute the absolute length of the edges. For this, we include the value in the column "oneway", indicating whether the edge is one-way or not. Then we derive out of those edges with a lane specification (that is, the column "lanes" is not "nan"), the average number of lanes. The average number of lanes per road classification are, in decreasing order: Trunk (7.3), primary (5.8), secondary (5.1), motorway (4.7), tertiary (4.0), unclassified (3.7), residential (2.7), living_street (2.5), other (1.7). The lane-kilometres per road classification is the product of the average number of lanes by the absolute length of the edges. The sum of all considered road classifications is then our estimate of the car network length in lane kilometres $L_{c,y}$ in year y.

It is important to note that the networks in OSM experience an increasing level of specification. In 2015, only 7.4% of edges in the car network had a lane specification, while in 2023, it increased to 41.7%. Additionally, the number of edges classified as "unclassified" decreased significantly by 67.0%, while edges with other edge classifications stayed at about the same level. As for the bike network, the edges in the bike network for which "cycleway" is defined is 71.5% in 2015 and 99.5% in 2023. The tag "oneway:bicycle" is specified for 0.3% of bike roads in 2015 and 41.2% in 2023. From those edges where it is specified, only few are specified as oneway: 2015 - 2017 it is 0.0%, meaning all cycleways which had this tag were two-ways. It rises to 11.1% in 2020 and drops to 1.6% in 2023. The increase in lane specification is likely due to quality improvements of OSM during the observation period. Nevertheless, this bias is potentially affecting the results of our analysis.

Network changes

In Figure 3, we can observe the relative changes of the car and bike network. The relative changes of car lane-kilometres differentiated by their road classification are depicted in blue and grey tones, and bike kilometres over the observation period are in pink.

Notably, the lane-kilometres of unclassified streets have decreased significantly by approximately 70%, undoubtedly a result of improved data over time. Additionally, there is a slight decrease in lanes classified as "secondary", "tertiary", and "other". On the other hand, there is a slight increase in lanes classified as "residential", while lanes classified as "primary and "trunk" appear to remain relatively stable.

Overall, the network's lane-kilometres have decreased from 10,759 km in 2015 to 10,237

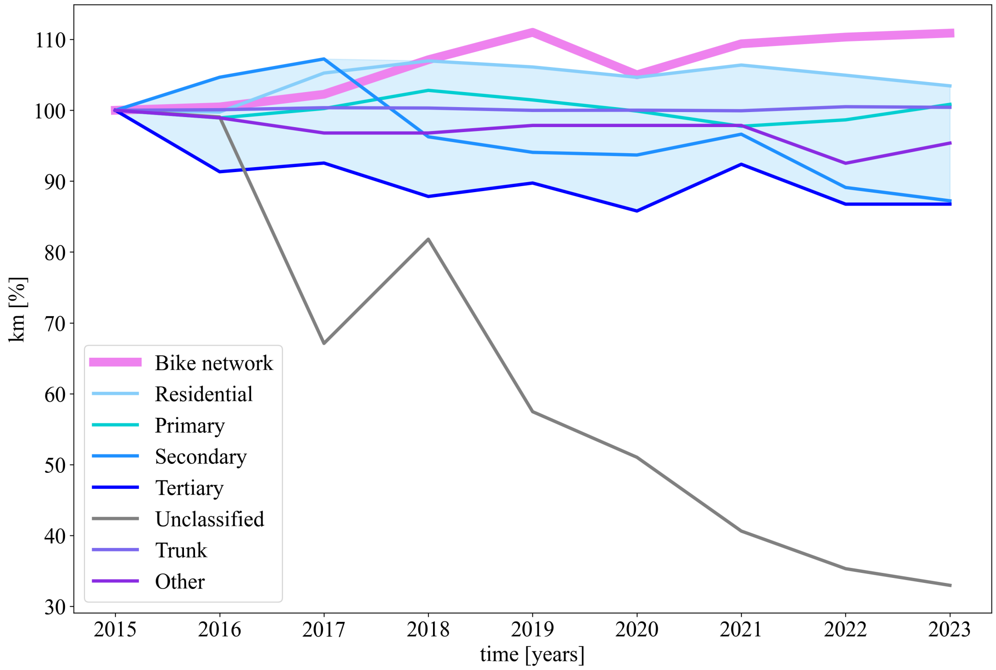

FIGURE 3 : Change of lane-kilometres, relative

km in 2023, representing an overall “space” decrease of 4.9%. The bike network has grown from 1,073 km in 2015 to 1,190 km in 2023, a 10.9% increase over the last eight years. For bikes, we do not carry out investigations regarding different cycleway classifications because the network is not sufficiently informative.

TRAFFIC DATA

To assess demand shifts, we analyze traffic data provided by official sources (*32, 33*). We use loop detector data from Paris for our analysis. Our focus lies on weekdays and the time range between 5 am to 11 pm, as the traffic data on weekends, holidays, and during the night is not relevant for assessing the long-term changes. We refer to those hours as “relevant hours”.

We analyzed the network data for January 1st from 2015 to 2023. However, when examining traffic data, we focus on complete calendar years, selecting representative days from each season. To maintain consistency, our analysis covers the years 2015 to 2022, as 2023 is ongoing.

Vehicle traffic data

Within the vehicle traffic dataset, we have 2,706 loop detectors available. However, only 33% of these detectors consistently provide at least one value for q and o each year from 2015 to 2023. Figure 4 depicts their availability over the years, with detectors that do not deliver any data for q and o in a given year filtered out. Figure 4 clearly reveals that not all detectors offer full coverage during the relevant hours. Notably, detectors that provide q and c for at least one relevant hour often demonstrate consistent data for a substantial portion of the relevant hours. However, these hours may not necessarily overlap.

Due to this limitation, we cannot utilize the complete data from all detectors on all days. We must reduce the sample by selecting a subset of detectors and days that offer data consistently

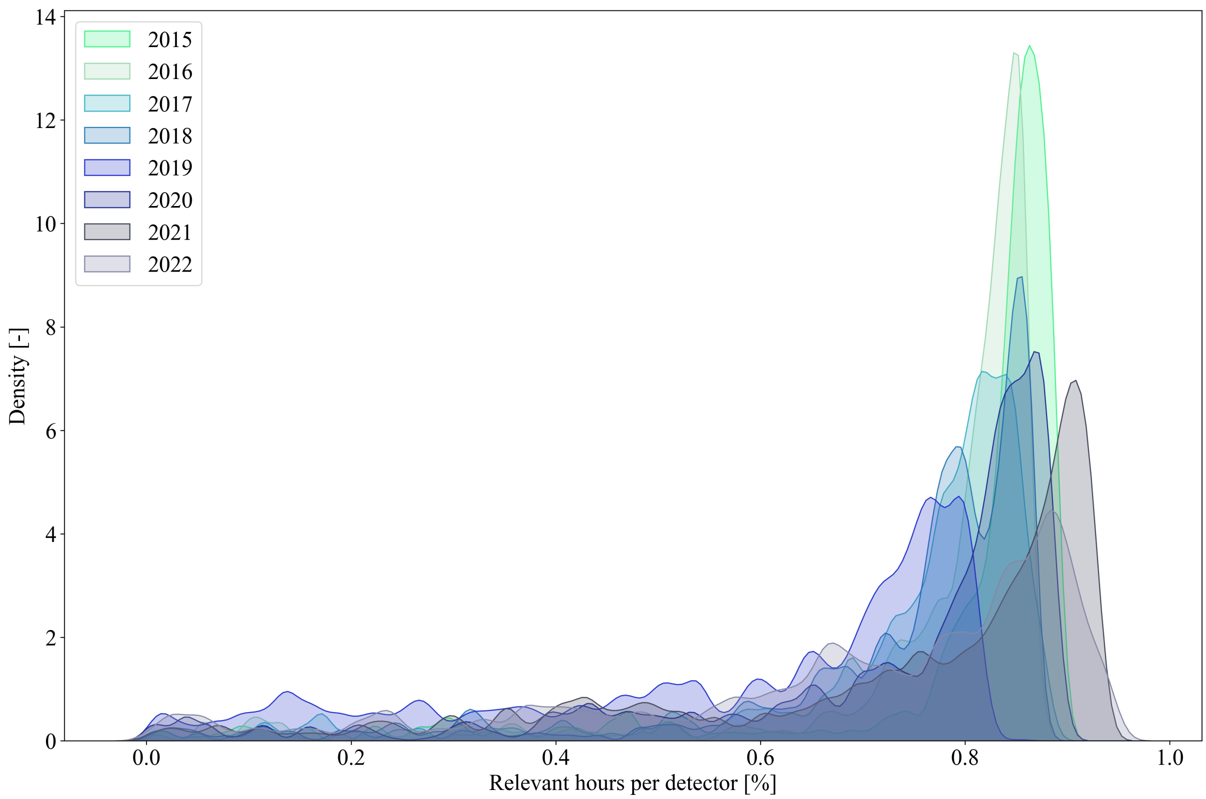

FIGURE 4 : Percentage of relevant hours per detector

every year and during the relevant hours of the day.

To achieve this, we proceed with the following methodical approach, see below. As a result, we identify a subset of 153 detectors, each covering the same 20 days per year. Note that in Paris one detector in the data reports data per road segment, not lane, i.e., it provides an aggregated measurement of several lane detectors. Figure 5 showcases the selected detectors, which cover 5.5% of Paris' road network (in 2023, there are 2,779 detectors). This process ensures that we work with reliable and comprehensive data, allowing for more accurate analysis and insights.

Methodological approach

Given a vehicle detector ψ, the *flow* q of ψ is the number of vehicles passing ψ per hour. The *occupancy* o of ψ is the percentage of the time that ψ is occupied with vehicles. We say that a work day φ is *vehicle-complete* for a detector ψ, if ψ measured both q and o for every hour between 5 am - 11 pm of φ.

In our analysis, we focus on a carefully chosen subset of detectors, which consists of precisely five vehicle-complete days per season. Each season includes one Monday, three days from Tuesday to Thursday, and one Friday. We standardized these vehicle-complete days across all detectors for consistency. To identify the largest possible subset meeting these criteria, we executed the following steps:

1. We start with 2,706 detectors in the geographical region, valid during our observation period and present in both the network (QGIS) and traffic data.
2. After filtering for relevant hours and making the dataset complete, we found that 48% -

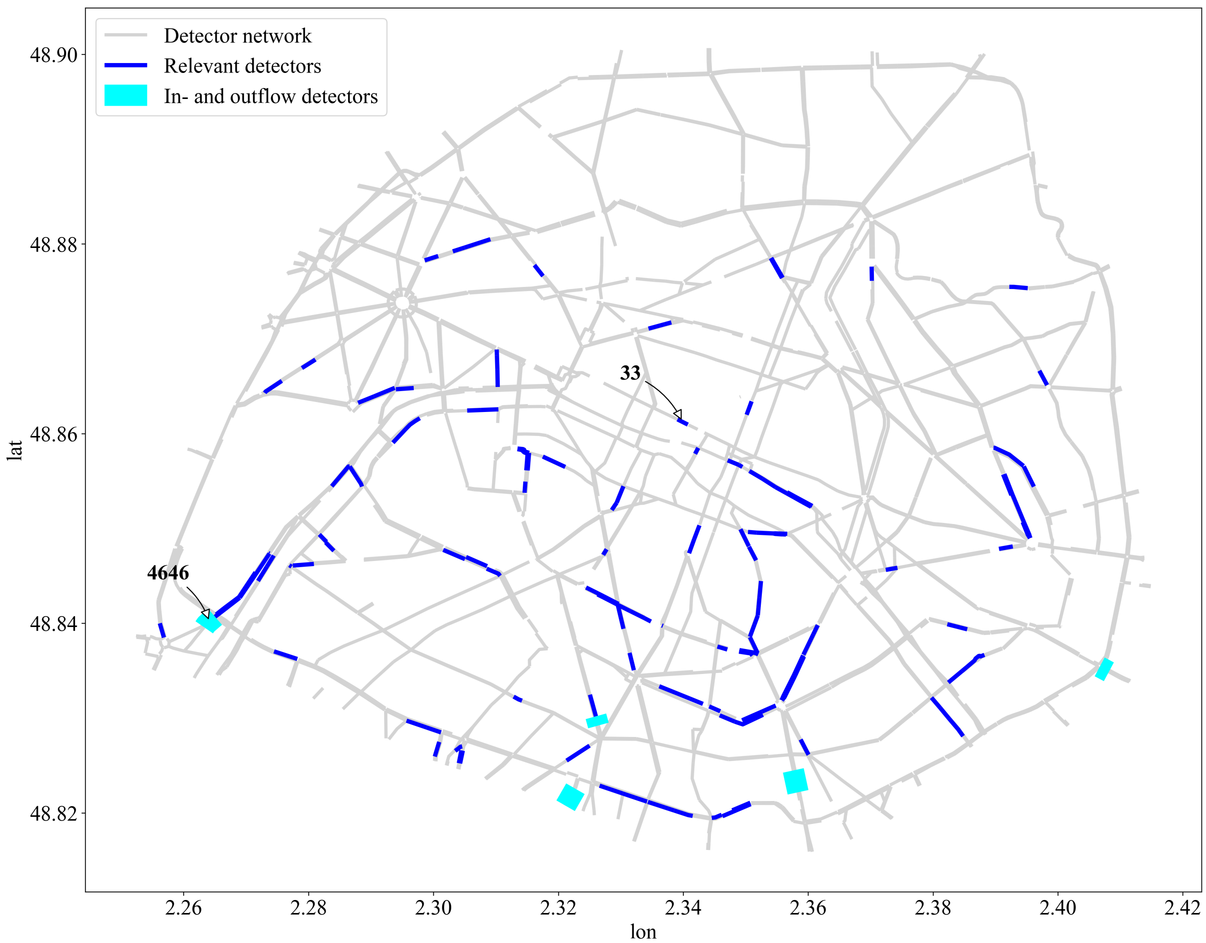

FIGURE 5 : The network and inflow vehicle detectors

61% of detectors provided data for at least one relevant hour, depending on the year.

3. Out of 2,706 detectors, 906 (33%) provided data for q and o for at least one hour every year. The data availability for these detectors is depicted in Figure 4.
4. Using nonlinear optimization, we identified 153 detectors measuring the same 299 vehicle-complete days.
5. We selected 20 days per year from the 299 vehicle-complete days, leaving us with 160 days.
6. After excluding days affected by COVID-19 and a high-risk incident, we obtained 154 *chosen vehicle-complete days*.

To explore the changes in traffic entering and leaving the city, we focus on the in- and outflow detectors, marked in cyan on Figure 5.

Figure 6 presents the traffic flow (q) for two detectors, displayed as raw data over all days. Notably, the inflow detector 4646 shows a consistent flow, remaining fairly stable over time. The network detector 33 exhibits a sharp decline over the years, suggesting changes on the supply side, e.g., a reduction in the number of lanes.

Both the consistent flow and the sharp decline are representative of the other network and

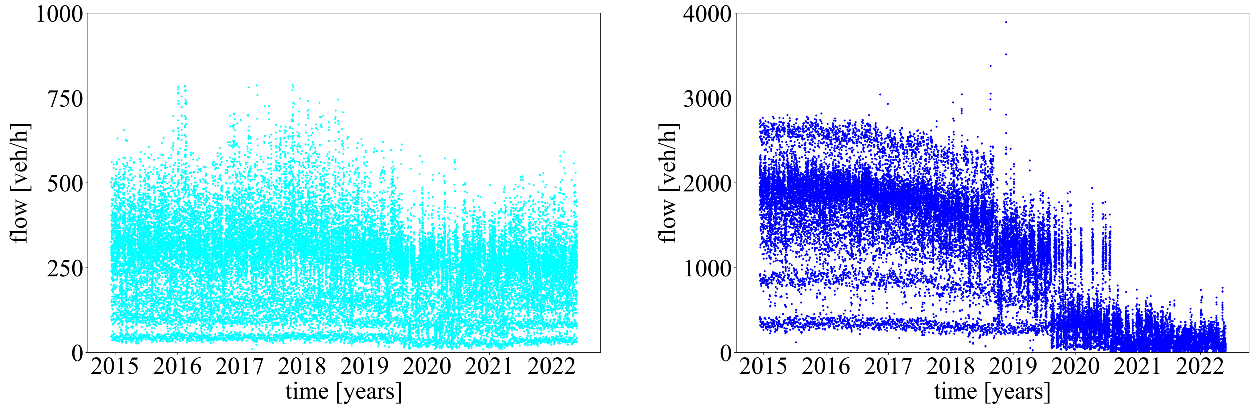

(a) Inflow detector 4646

(b) Network detector 33

FIGURE 6 : Vehicle traffic over time

inflow detectors.

Bike traffic data

The city of Paris installed bike traffic detectors from 2016 onwards, totaling 73 distinct detectors. To directly compare bike traffic to vehicle traffic, we aimed to consider days for which we analyzed vehicle traffic. However, no single bike detector delivered data for all relevant hours of the chosen vehicle-complete days (from 2016 onwards).

As the number of bike detectors is limited, selecting detectors and complete days like we did for vehicle traffic isn't feasible. We relaxed the criterion to consider bike detectors "valid" for a given year if they had bike counts for every relevant hour on at least $n-10$ days out of n vehicle-complete days. This led to the following distribution:

1. 6 detectors are valid 2016 - 2023
2. 23 detectors are valid 2019 - 2023
3. The rest of the detectors (44) do not deliver consecutive data

Our analysis focuses on detectors in groups 1 and 2. Figure 7 displays the selected detectors, covering 9.5% (2016-) / 36.5% (2019-) of Paris' bike network (in 2023, 63 detectors are present).

The detectors, especially those installed first (in purple), are at central spots of the bike network. Detectors installed in 2019 are also positioned centrally, depicted in violet. Some detectors are close to each other or overlap, like four of the six detectors in group 1.

Figure 8 displays bike counts from two detectors in each group 1 and 2, showing raw data across all days. The plots reveal a gradual increase in bike traffic over time, with a noticeable dip in 2020, likely attributable to COVID-19. These patterns are representative of other bicycle detectors in groups 1 and 2.

RESULTS

We present the results as follows. First, we present the network changes, i.e., the supply side, then we present the traffic flow changes, i.e., the demand side, before combining both.

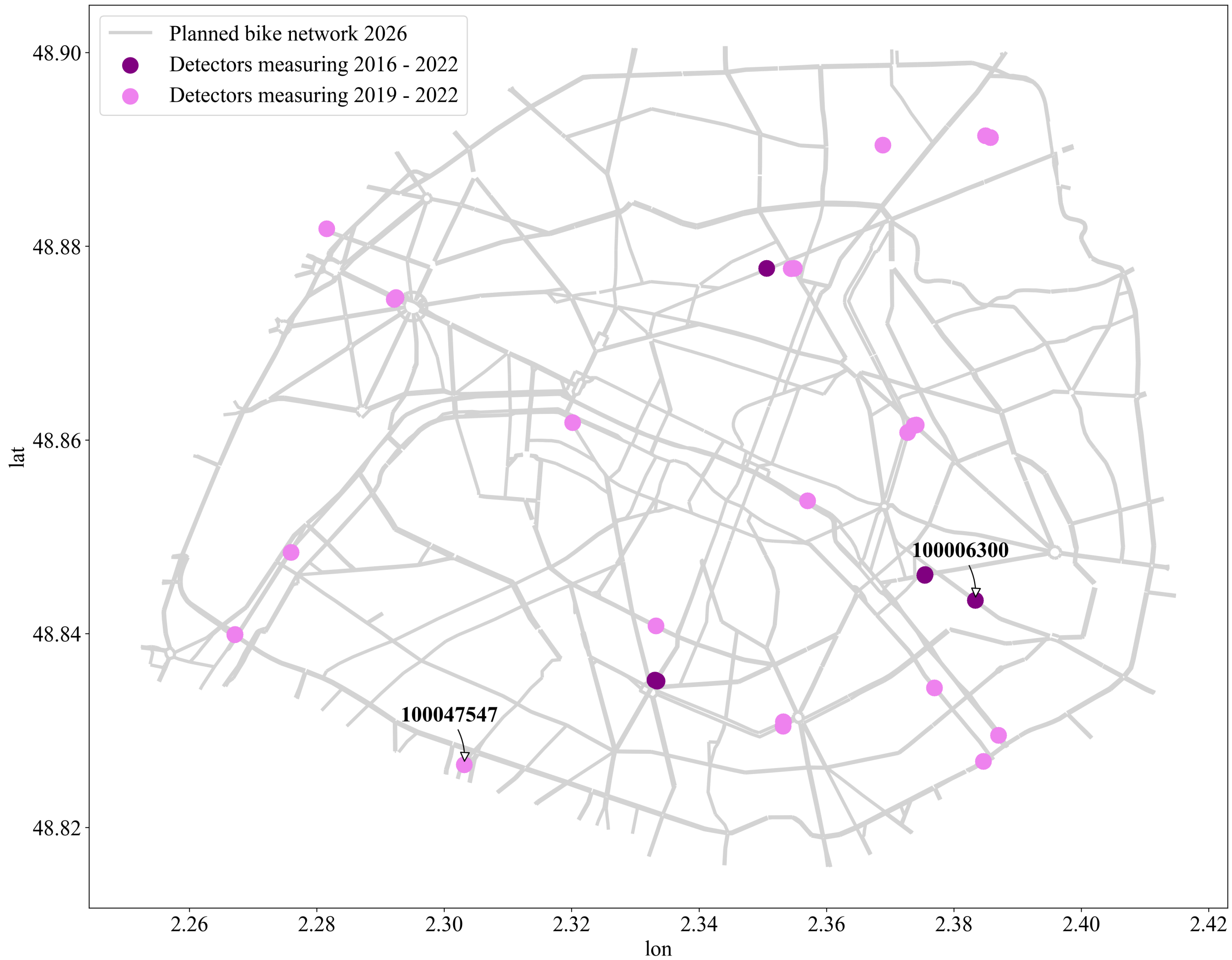

FIGURE 7 : Planned bike network 2026 within study area, with detectors

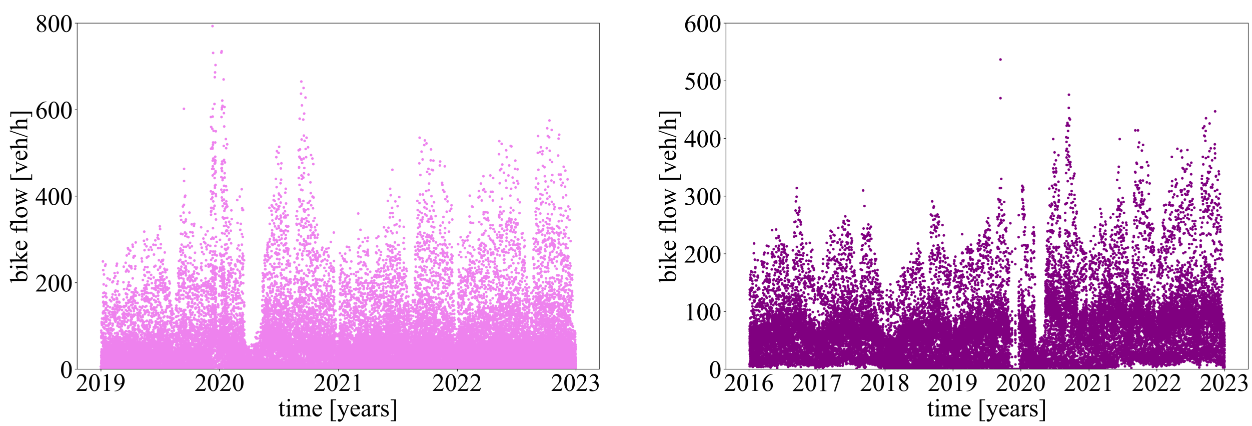

(a) Detector 100047547

(b) Detector 100006300

FIGURE 8 : Bike traffic over time

Supply-side changes

In Figure 9, we show the estimated MFDs for the years 2015 and 2022. Recall that we defined the capacity as the 95th percentile of the travel production. It can be seen that from 2015 to 2022, the capacity is reduced by 14.9%, while the observed average accumulation of vehicles is reduced by 15.3%. The reduced capacity can be explained by the network measures that reduced the available space for cars. If there had been no change in car travel demand, the MFD in 2022 would exhibit higher accumulation levels and likely a more distinct congestion branch; however, this is not observed, suggesting that car travel demand adapted, e.g., by changing mode, departure time, or conducting no trip at all. Additionally, the observed free-flow branch in the MFD suggests that some network measures led to a decrease in free-flow speed and created a more substantial bending of the curve (in MFD terms, the slope of the second cut is less in 2022 compared to 2015). Possible explanations for this observed behavior are reduced free-flow speeds, changes to traffic control, and more moving bottlenecks.

In Figure 10, we combine the changes in capacity with the changes in car and bike network length. The capacity, plotted in grey, shows a 2.8% initial increase in 2016, followed by a continuous decrease starting from 2017. By 2022, there's a reduction of 14.9% compared to the 2015 value. It can be seen that the observed capacity decreased more than the total network length for cars. This gap suggests that either the used data is biased, e.g., the selected subset of links is not representative or the data in OSM is incomplete, or that there are further unobserved factors that decreased the MFD capacity stronger than the network length, e.g., changes to traffic control or speed limit changes.

Demand-side changes

Figure 11 illustrates the changes in traffic flow, i.e., observed travel demand, as measured in travel production $\bar{\Pi}_y$, inflow travel production $\bar{\Pi}_{y,inflow}$, and the average accumulation of vehicles $\bar{n}_y$. It is evident that these metrics follow similar patterns: a slight increase until 2017, a decrease in 2020 (likely due to the impact of COVID-19), followed by another slight increase. However, as of 2022, it is notable that travel production, inflow, and average network accumulation are all below 2015 levels. The traffic flow inside and outside the city was monitored through five detectors positioned near the outer ring of the city, as depicted in Figure 5 in the traffic data section. In contrast, the behavior of bike demand exhibits different patterns: The purple line, representing detectors measuring bike traffic from 2016 onwards, shows a slight decline in 2018, followed by an increase in 2019, a relatively steady rise until 2020, and finally, an exponential increase from 2020 onwards. The detectors installed in 2019, depicted in violet, also demonstrate an exponential increase from 2020 onwards, but with a shallower curve. These variations in behavior can be attributed to the positioning of the detectors. The initial detectors were strategically placed at crucial locations within Paris' bike network. Consequently, it is reasonable to observe a steeper increase in bike traffic at these early installation locations compared to spots where detectors were installed later in the observation period.

Combining supply- and demand side changes

In Table 3, we summarize the overall changes in network (supply), traffic/travel (demand), and emissions. The car network experienced a reduction of 4.9% measured in lane kilometers, while the bike network increased 10.9% during the observation period. During this period, the observed MFD capacity decreased by 12.4%, and the average accumulation of vehicles decreased by 8.5%.

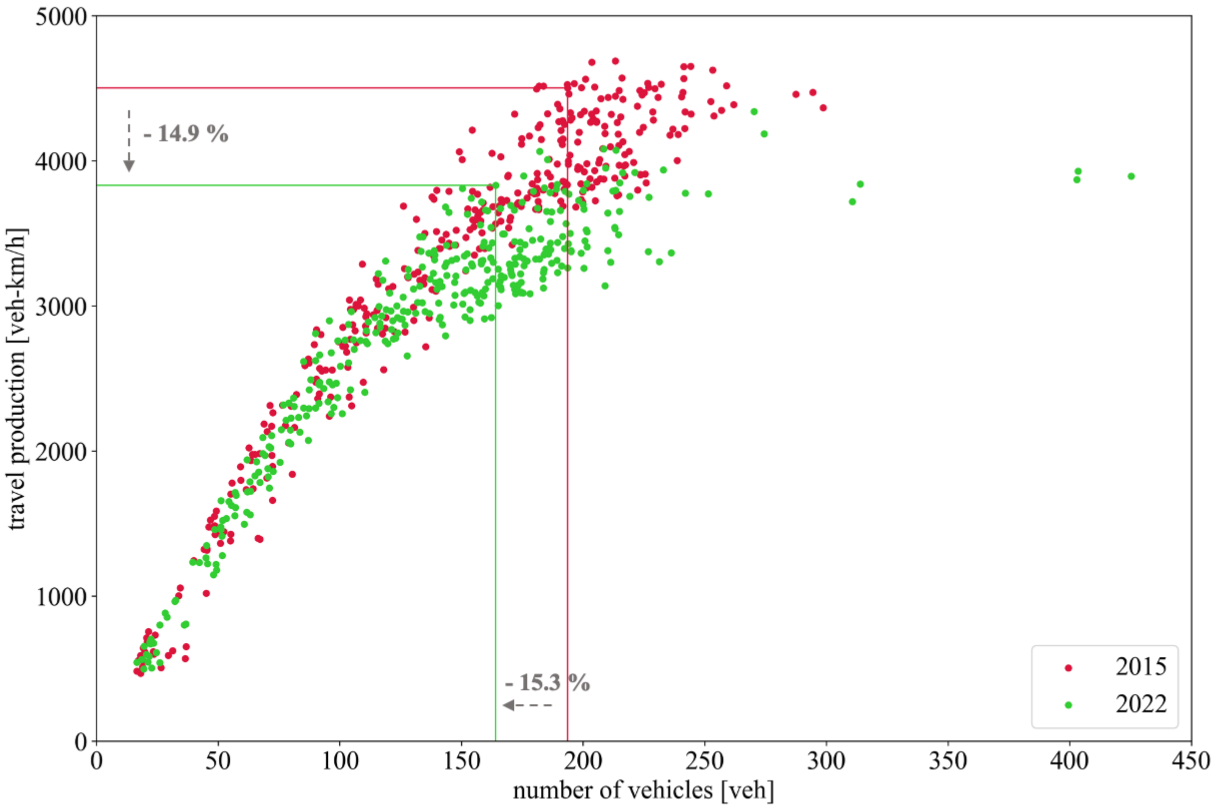

FIGURE 9 : MFD for the years 2015 and 2022

The travel production declined by 13.4%, and the inflow travel production decreased by 23.4%. Conversely, bike traffic exhibited substantial growth. Detectors from 2019 onwards observed a 57.1% increase (2019 - 2022). For detectors starting in 2016, the increase was even more pronounced: The change was 73.6% for 2019 - 2022 and 93.9% for 2016 - 2022.

In Figure 12, we present a comparison of changes on the supply side with changes on the demand side, specifically examining the MFD capacity in relation to network travel production, inflow travel production, and average network accumulation. The data reveals a positive correlation between the supply and demand measures. Both travel production and congestion levels have decreased, contradicting the hypothesis based on the Downs/Thomson paradox, which suggests that travel production reductions should result in similar congestion levels before and after the intervention. The observed reduction in congestion is significant, indicating that additional unobserved

TABLE 3 : Summary of relative changes from 2015 to 2022

	Changes from 2015 to 2022 (%)		
Mode	Network (supply side)	Traffic/travel (demand side)	Emissions
Vehicle	-4.9%	-13.4% [network d.] / - 23.4% [inflow d.]	-11.4%
Bike	+10.9%	+93.9% [2016-] / +57.1%, +73.6% [2019-]	0%

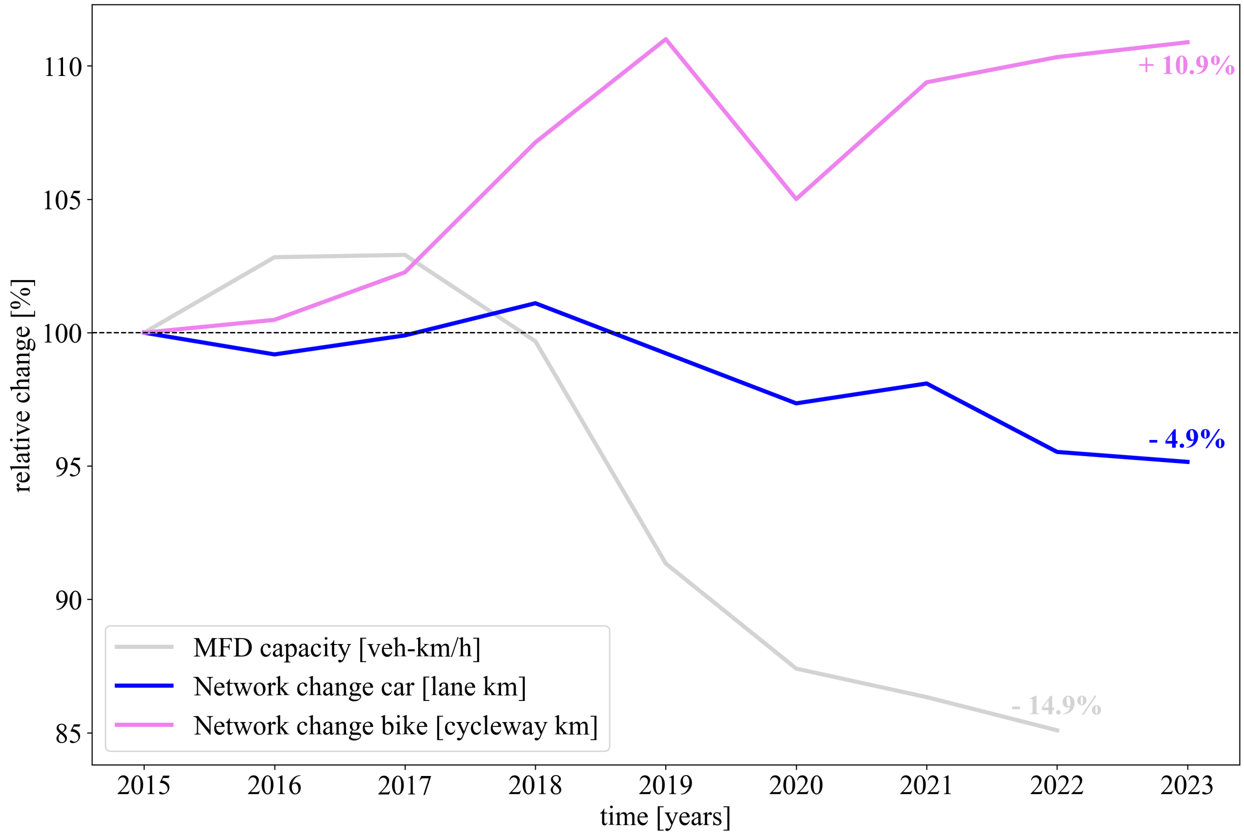

FIGURE 10 : Change of network and MFD capacity over time

factors, such as remote work practices, likely contribute to the observed changes.

Assessment of changes in carbon emissions

Based on the estimated MFD (see Figure 9) and speed-specific emission factors (see Table 2), we analyzed the average daily emissions in the specific sub-network defined by the loop detector links (Figure 5). The results, as shown in Figure 13, consider both car travel production and associated speed, as per the emissions-MFD (*22*). Over the period from 2015 to 2022, a notable reduction of 11.4% in carbon emissions was observed for our selected subnetwork.

The chosen subnetwork can be considered a reliable proxy for the broader Paris area. Consequently, the estimated emission reduction in this subnetwork provides a close approximation of the overall emission reduction for the entire region.

DISCUSSION

The analysis of the relationship between supply-side changes in the network and demand-side changes in traffic flow and travel production using the macroscopic fundamental diagram (MFD) and emission-MFD shows that the supply-side measures coincided with changes on the demand side, leading to a substantial reduction in carbon emissions from car traffic. However, a reduction in car travel by the Downs/Thomson paradox was not supported by the data. This section discusses the methods, data, and findings.

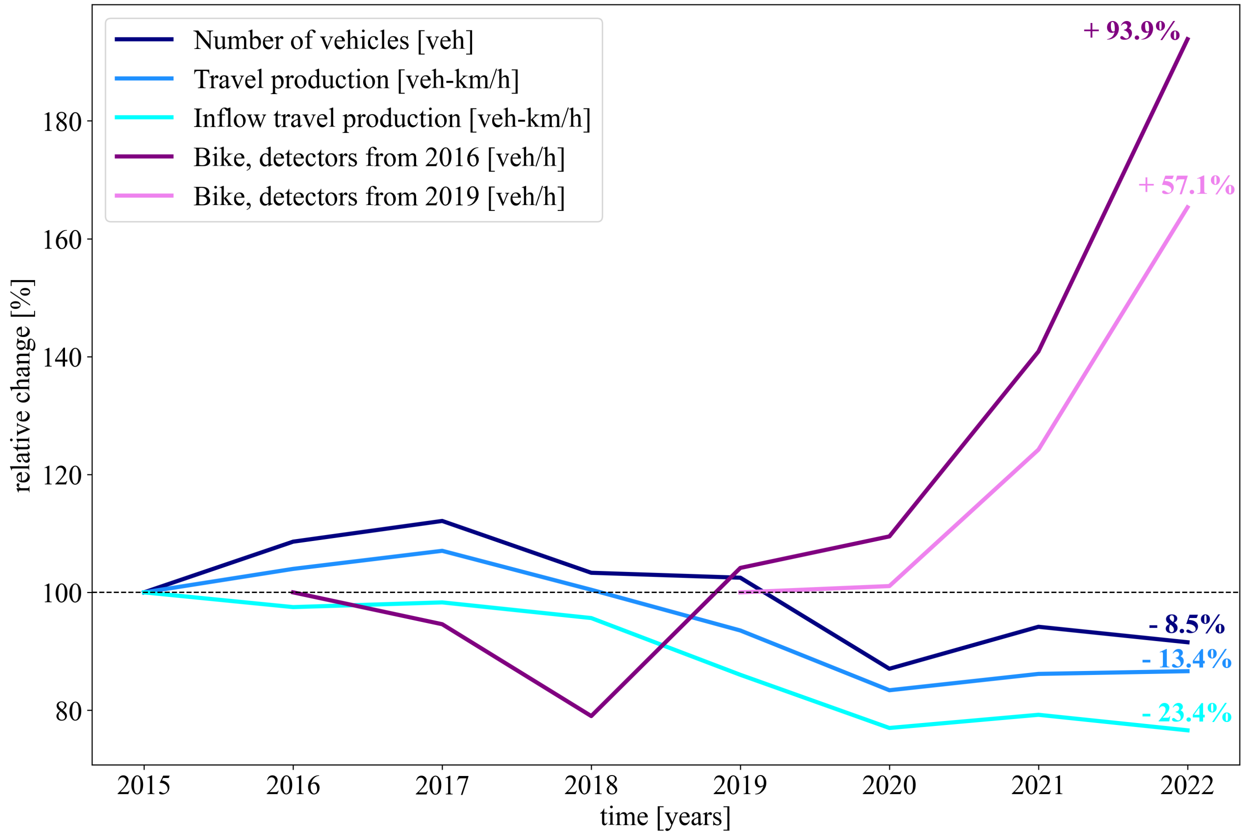

FIGURE 11 : Demand changes

Methods

Our study uses the MFD and the emission-MFD as key methods. Here, the MFD estimation can be improved by fusing loop detector with floating car data (*34*) as well as partitioning of the network (*35*). Further, our present analysis does not takes into account trip lengths, which is a key parameter to transform travel production into trip rates (*13*). To enhance our analysis, we can also employ methods to estimate origin-destination matrices from the loop detector data (*36*) to estimate the trip production and its development over time.

Further, considering estimates of door-to-door travel times for public transport and cycling could improve the assessment of whether the Downs/Thomson paradox determines the new observed congestion levels in the city or not.

Data

The information provided by OpenStreetMap does not entirely reflect the actual road network; Further, data quality improved substantially during the observation period. In particular, OpenStreetMap lacks precise specifications for the road classification as well as how many lanes each road segment has. Additionally, there is a time lag in data updates, as changes are not immediately documented. This affects both modes, car and biking. Unfortunately, we could not corroborate the numbers from OpenStreetMap with official data.

Regarding traffic data, it is surprising that only 153 out of over 2,700 detectors reported several full days throughout the observation period. Increasing the coverage of loop detectors in

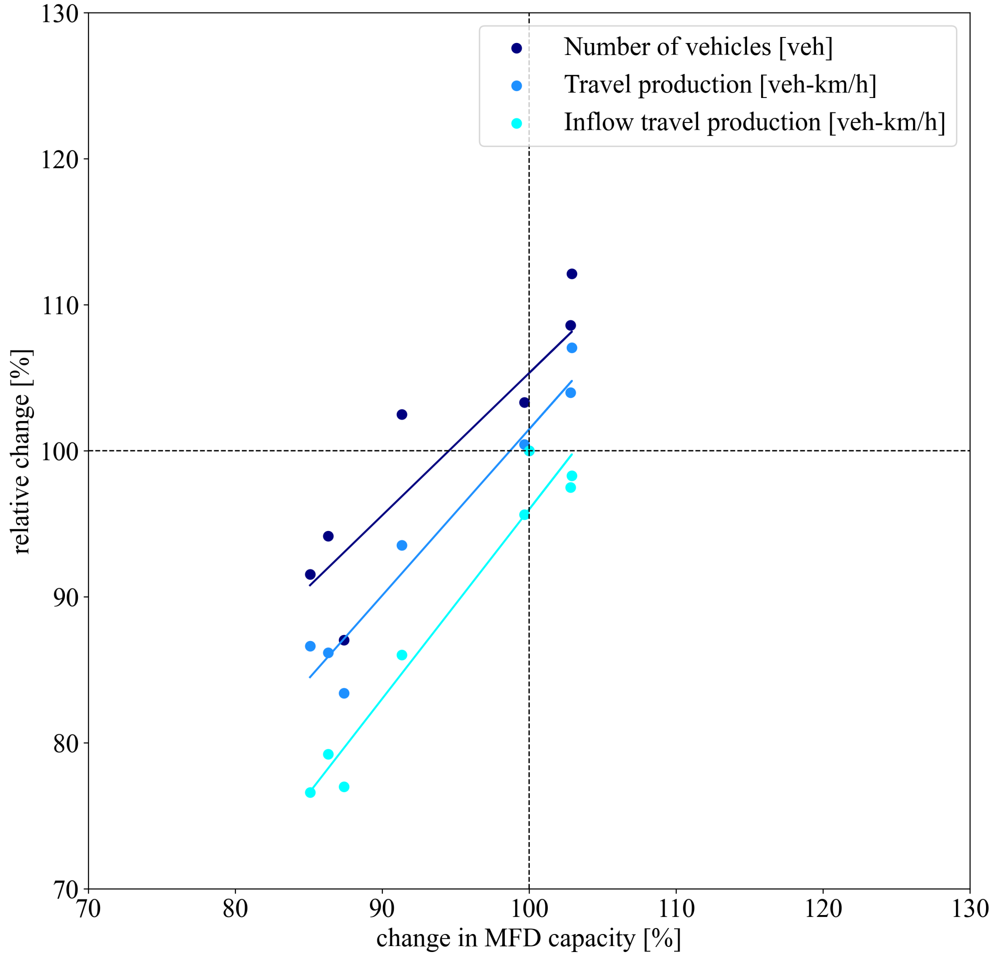

FIGURE 12 : Relative changes to MFD capacity

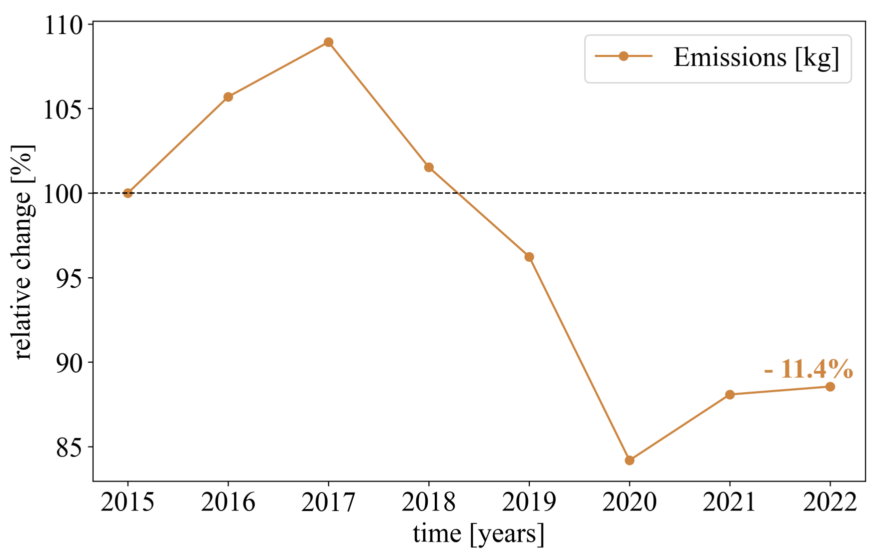

FIGURE 13 : Emission development

the analysis and MFD estimation could help to reduce a likelihood of a loop detector selection bias. Further, obtaining precise information on the number of lanes at the measurement location would improve the estimation of travel production; this information, together with better speed information for MFD calibration, would also help to investigate whether the occupancy scale has a similar interpretation each year.

Findings

The relationship between changes in the network supply and changes in traffic with subsequent impacts on carbon emissions is intuitive and aligns well with Paris' policy objective. Importantly, the macroscopic perspective of the MFD does not inform about individual-specific reasons, e.g., working from home or peak avoidance. Nevertheless, data reveals that congestion levels in Paris declined from 2021 to 2022 (*25*), which corroborates our findings based on the MFD in Figure 11.

A throughout assessment of the policy measure requires the consideration of more dimensions. For example, the health benefits of cycling or reducing the urban heat island effect by greening more urban space. This investigation is only an interim assessment of the fundamental changes in Paris. It will be particularly interesting to study traffic behavior once the changes are fully implemented.

CONCLUSION

In this paper, we explored the relationship between network changes and traffic for both bike and car in Paris from 2015 to 2022. We analyzed the impact on carbon emissions reduction from vehicle traffic using empirical data. Travel production declined by 13.4%, while inflow travel production decreased by 23.4%. In contrast, bike traffic increased significantly, with a 57.1% rise for detectors measuring from 2019 onwards and a more substantial 93.9% increase for detectors measuring from 2016 onwards. Over the same period, the car network length decreased by 4.9%, while the bike network expanded by 10.9%. Interestingly, the MFD capacity decreased by 14.9%, suggesting other factors influencing network performance. In conclusion, these changes collectively led to an 11.4% reduction in carbon emissions from vehicle traffic between 2015 and 2022.

The focus of future research is on improving the data quality from both network and traffic recordings; presumably, integrating another source like floating car data. Additionally, a throughout economic assessment of the changes of all relevant internal and external costs should be undertaken to evaluate the effectiveness of Paris' policy of re-adapting its road-based transportation system.

The benefits of the transformation in Paris are not limited to carbon savings alone. It is conceivable that the mode shift towards cycling could also have implications for the health of citizens and urban greening. Paris is a prominent and most likely successful example of efforts to reduce carbon emissions from transportation by managing demand and not technology alone. Consequently, one can conclude that the changes in Paris provide valuable insights that could apply to other metropolises too.

ACKNOWLEDGMENTS

Allister Loder acknowledges funding by the Bavarian State Ministry of Science and the Arts in the framework of the *bidt* Graduate Center for Postdocs. Elena Natterer acknowledges funding from the research project MINGA by the German Ministry for Digital and Transport.

AUTHOR CONTRIBUTIONS

The authors confirm contribution to the paper as follows: study conception and design: Elena Natterer, Allister Loder, Klaus Bogenberger; data collection: Elena Natterer; analysis and interpretation of results: Elena Natterer, Allister Loder; draft manuscript preperation: Elena Natterer. All authors reviewed the results and approved the final version of the manuscript.

GPT-3 assisted in summarizing paragraphs.

References

1. Forbes: France will spend 2 billion to double bike lanes expand cycling, 2023.
2. City of Paris: Carbon Neutral by 2050 for a Fair, Inclusive and Resilient Transition | France, 2023.
3. Buehler, R. and J. Pucher, Cycling through the COVID-19 pandemic to a more sustainable transport future: Evidence from case studies of 14 large bicycle-friendly cities in Europe and North America, 2022.
4. Plan Velo I, 2023.
5. Plan Velo II, 2023.
6. Why Paris is eliminating 72 percent of its on-street parking spaces, 2023.
7. O'Sullivan, L., Feargus; Bliss, The 15-Minute City—No Cars Required—Is Urban Planning's New Utopia, 12 November 2020, retrieved 29 March 2021.
8. Downs, A., The law of peak-hour expressway congestion. *Traffic Quarterly*, Vol. 16, No. 3, 1962, pp. 393–409.
9. Mogridge, M. J. H., The self-defeating nature of urban road capacity policy. *Transport Policy*, Vol. 4, 1997, pp. 5–23.
10. Mogridge, M. J. H., D. J. Holden, J. Bird, and G. C. Terzis, The Downs/Thomson paradox and the transport planning process. *International Journal of Transport Economics / Rivista internazionale di economia dei trasporti*, Vol. 14, No. 3, 1987, pp. 283–311, publisher: Accademia Editoriale.
11. Less is more: Changing travel in a post-pandemic society, 2023.
12. Barrero, J. M., N. Bloom, and S. J. Davis, *Why Working from Home Will Stick*. Working Paper 28731, National Bureau of Economic Research, 2021.
13. Daganzo, C. F., Urban gridlock: Macroscopic modeling and mitigation approaches. *Transportation Research Part B: Methodological*, Vol. 41, No. 1, 2007, pp. 49–62.
14. Geroliminis, N. and C. F. Daganzo, Existence of urban-scale macroscopic fundamental diagrams: Some experimental findings. *Transportation Research Part B: Methodological*, Vol. 42, 2008, pp. 759–770.
15. Daganzo, C. F. and N. Geroliminis, An analytical approximation for the macroscopic fundamental diagram of urban traffic. *Transportation Research Part B: Methodological*, Vol. 42, 2008, pp. 771–781.
16. Laval, J. A. and F. Castrillón, Stochastic approximations for the macroscopic fundamental diagram of urban networks. *Transportation Research Part B: Methodological*, Vol. 81, No. 3, 2015, pp. 904–916, publisher: Elsevier B.V.
17. Loder, A., L. Ambühl, M. Menendez, and K. W. Axhausen, Understanding traffic capacity of urban networks. *Scientific Reports*, Vol. 9, No. 16283, 2019.

18. Geroliminis, N., N. Zheng, and K. Ampountolas, A three-dimensional macroscopic fundamental diagram for mixed bi-modal urban networks. *Transportation Research Part C: Emerging Technologies*, Vol. 42, 2014, pp. 168–181.
19. Dantsuji, T., D. Fukuda, and N. Zheng, Simulation-based joint optimization framework for congestion mitigation in multimodal urban network: a macroscopic approach. *Transportation*, Vol. 48, No. 2, 2021, pp. 673–697, publisher: Springer US ISBN: 0123456789.
20. Ortigosa, J., V. V. Gayah, and M. Menendez, Analysis of one-way and two-way street configurations on urban grid networks. *Transportmetrica B: Transport Dynamics*, Vol. in press, 2017, pp. 1–21, publisher: Taylor & Francis.
21. Loder, A., M. C. Bliemer, and K. W. Axhausen, Optimal pricing and investment in a multimodal city — Introducing a macroscopic network design problem based on the MFD. *Transportation Research Part A: Policy and Practice*, Vol. 156, No. January, 2022, pp. 113–132.
22. Barmpounakis, E., M. Montesinos-Ferrer, E. J. Gonzales, and N. Geroliminis, Empirical investigation of the emission-macroscopic fundamental diagram. *Transportation Research Part D: Transport and Environment*, Vol. 101, 2021, p. 103090.
23. Leclercq, L., N. Chiabaut, and B. Trinquier, Macroscopic fundamental diagrams: A cross-comparison of estimation methods. *Transportation Research Part B: Methodological*, Vol. 62, 2014, pp. 1–12.
24. Knoop, V. L., *Introduction to Traffic Flow Theory*. Delft University of Technology, Delft, The Netherlands, 2nd ed., 2018.
25. TomTom, *Paris Traffic*, 2023, https://www.tomtom.com/traffic-index/paris-traffic/.
26. Daganzo, C. F., *Fundamentals of Transportation and Traffic Operations*. Pergamon, Oxford, 1997.
27. Open Street Map, 2023.
28. Boeing, G., OSMnx: New Methods for Acquiring, Constructing, Analyzing, and Visualizing Complex Street Networks. *Computers, Environment and Urban Systems 65, 126-139.*, 2017.
29. Open Street Map, Key: Highway, 2023.
30. Open Street Map, Key: Cycleway, 2023.
31. Geoffrey Boeing suggests to consider a graph comprising everything with either a cycleway key or highway=cycleway, 2023.
32. Paris open data car traffic count, 2023.
33. Paris open data bicycle traffic count, 2023.
34. Ambühl, L. and M. Menendez, Data fusion algorithm for macroscopic fundamental diagram estimation. *Transportation Research Part C: Emerging Technologies*, Vol. 71, 2016, pp. 184–197.
35. Ji, Y. and N. Geroliminis, On the spatial partitioning of urban transportation networks. *Transportation Research Part B: Methodological*, Vol. 46, No. 10, 2012, pp. 1639–1656.
36. Yang, H., T. Sasaki, Y. Iida, and Y. Asakura, Estimation of origin-destination matrices from link traffic counts on congested networks. *Transportation Research Part B: Methodological*, Vol. 26, No. 6, 1992, pp. 417–434.